

INITIATION AND GROWTH OF SHORT CRACKS DURING CYCLING IN AN AGED SUPERDUPLEX STAINLESS STEEL

M. Balbi^{1, a}, S. Hereñú^{1, b}, I. Proriol Serre^{2, c}, J.-B. Vogt^{2, d}, A. F. Armas^{1, e} and I. Alvarez-Armas^{1, f}

¹ Instituto de Física Rosario, CONICET - Universidad Nacional de Rosario, Bv. 27 de Febrero 210 bis - Rosario – Argentina

²Unité Matériaux et Transformations, CNRS/ENSCL/USTL, UMR 8207, Université de Lille 1, 59655 Villeneuve d'Ascq cedex, France

^a balbi@ifir-conicet.gov.ar , ^b herenu@ifir-conicet.gov.ar , ^c ingrid.serre@univ-lille1.fr, ^d jean-bernard.vogt@ensc-lille.fr, ^e armas@ifir-conicet.gov.ar, ^f alvarez@ifir-conicet.gov.ar

Keywords: low-cycle fatigue, duplex stainless steels, short cracks initiation and propagation, aged material

Abstract. The kinetics of short crack growth during cycling has been studied in a superduplex stainless steel in aged condition. After few cycles, slip lines appear distributed in both phases but the preferred phase for microcrack nucleation is the ferrite. Contrary to the exponential behavior observed in the as-received material, the growth rate of microcracks in aged condition follows a rather linear law. Internal dislocation structures were studied in the near surface region; microbands that sometimes extend over several grains were found at approximately 45° of the tensile axis on ferrite grains. The origin of the microbands has been analyzed and correlated with the microcracks.

Introduction

Wrought duplex stainless steels (DSSs) are two-phase alloys based on the Fe-Cr-Ni system with approximately equal proportions of ferrite and austenite phases. These materials are used in the intermediate temperature range (about -60 to 300°C) where resistance to acids and aqueous chlorides is required. Early grades were alloyed with approximately 18% Cr, about 4-6% Ni, and sometimes with Mo. Current commercial grades contain between 22-26% Cr, 4-7% Ni, up to 4.5% Mo, 0.10-0.35% N, and 0.7% Cu and W, [1]. Continual modifications to the alloy compositions have improved corrosion resistance, workability, and weldability.

Although DSSs are regarded as high-potential industrial materials, they are susceptible to spinodal decomposition when exposed to temperatures between 300-500°C. The spinodal decomposition of the ferritic phase leads to higher hardness, yield stress and ultimate tensile strength, but it dramatically decreases ductility and toughness. Although the influence of spinodal decomposition on the mechanical properties of DSS under monotonic loading is well documented, it has been studied much less extensively under cyclic loading [2, 3]. Even fewer investigations have examined the evolution of the surface damage before microcracking begins [4, 5]. Recently, the kinetics of microcrack growth during cycling has been studied in aged DSS S32205. In this case, microtwins on the ferrite phase are responsible for crack initiation [6].

In order to elucidate the mechanisms of microcrack nucleation and propagation during cycling in aged DSS S32750, this work studies the surface damage evolution and correlates it with the internal dislocation structure.

Experimental Procedure

The material studied in this investigation is the superduplex stainless steel type S32750 manufactured in the form of hot-rolled and solution annealed (as-received) cylindrical bars. The structure of the steel is composed of islands of austenite elongated in the rolling direction embedded

in a ferritic matrix. The material was studied in two different thermal conditions: as-received and aged 475°C for 100 h but in the present paper only the results in the aged condition were presented. **Fig. 1** is the optical micrograph of a section parallel to the bar axis in the as-received condition. The volume fraction of austenite is approximately 50% and the average austenitic grain size in the plane perpendicular to the specimen axis is about 10 μm .

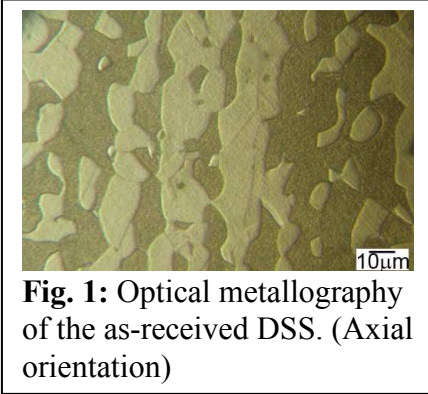


Fig. 1: Optical metallography of the as-received DSS. (Axial orientation)

Cylindrical specimens of 8.8 mm in diameter and 20 mm in gauge length were manufactured and polished in the test section to achieve a smooth surface. These specimens were used to obtain the cyclic stress–strain curves and the fatigue lifetime for both thermal conditions, as-received and aged. Additionally, studies on micro-cracks initiation and growth during fatigue were carried out on slightly shallow-notched cylindrical specimens [6]. The notch focuses the fatigue damage in the zone of observation, (stress concentration factor is 1.06 at the notch tip). Mechanical and electrolytical polish was given to the surface of the shallow notch to improve the

observation of micro-crack nucleation and growth. The central part of the notch was monitored during the test using a powerful optical system consisting of a CCD camera JAI mod. CM-140MCL with an objective of 50X, $\pm 1\mu\text{m}$ FD and 13mm WD and a 12X ultra zoom.

The tension/compression low-cycle fatigue tests were performed at room temperature on an electromechanic testing machine INSTRON mod. 1362. The tests were carried out under plastic strain control with a fully reversed triangular wave at constant plastic strain range of 0.3% and total strain rate of $2 \times 10^{-3} \text{ s}^{-1}$. At the beginning of the test, the machine was stopped at increasing intervals starting from 10 or 20 cycles and then each 150 cycles until the rupture. The crosshead of the machine was stopped in tension at 80% of the maximum tensile stress corresponding to the selected cycle to record the damage on the surface of the shallow notch. In a similar test, the true length of the crack advancing into the interior of the specimen, perpendicular to the tensile axis was estimated using the heat tinting method [6].

In the present work, the surface relief and the dislocation structure were evaluated after testing by scanning electron microscopy (SEM), atomic force microscopy (AFM) and transmission electron microscopy (TEM). The used AFM is a Digital III Atomic Force Microscope in tapping mode with a Veeco anisotropic pyramidal tip MPP-11100 (front angle 15° , back angle 25° , side angle 17.5° and radius of curvature inferior to 10nm).

Results and Discussion

Mechanical Test. Fatigue life has been measured on standard smooth cylindrical specimens in the

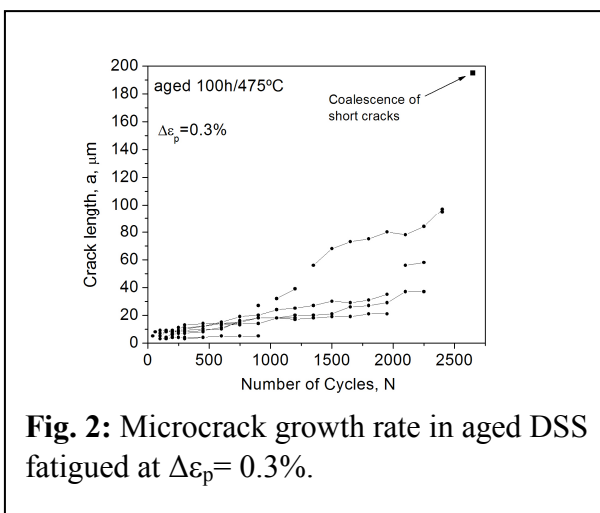


Fig. 2: Microcrack growth rate in aged DSS fatigued at $\Delta \epsilon_p = 0.3\%$.

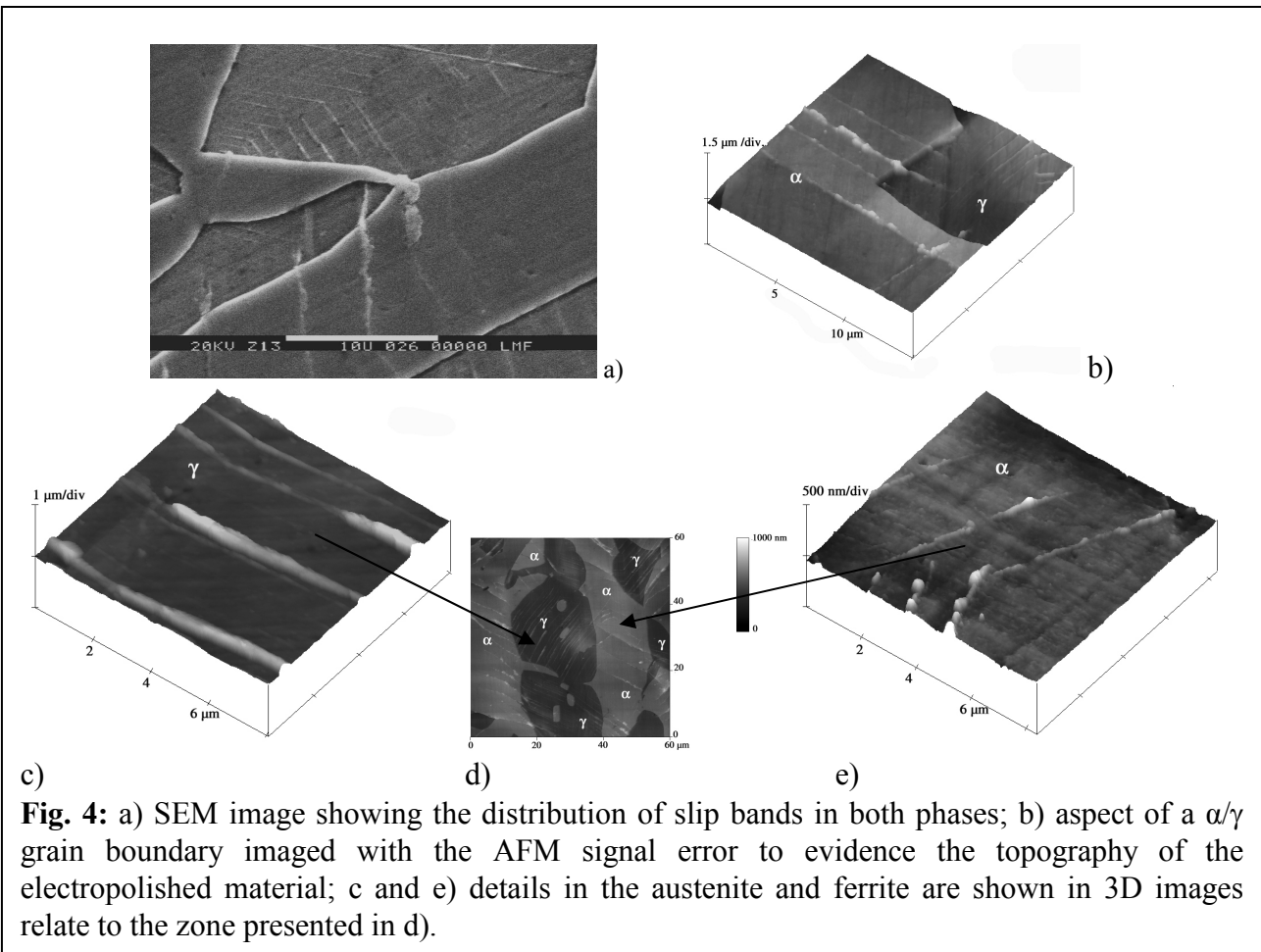
as-received and in the aged conditions subjected to constant plastic strain range of 0.3%. The fatigue life in both conditions is very close with an uncertainty of 10%. The microcrack nucleation and propagation has been studied in the shallow-notched specimens in both thermal conditions. In the aged material microcracks nucleate at persistent slip markings in the ferritic phase. **Fig. 2** shows the evolution of several microcracks that will give rise to one dominant effective short fatigue crack. This dominant crack is formed with the contribution of numerous microcracks of 100 μm in length. All of them grow linearly with the number of cycles and almost at the same rate.

Additionally, phase boundaries do not act as crystallographic barriers. The microcracks pass through these barriers without any decrease in velocity.

TEM Observations. A planar arrangement of dislocations, similar to that observed in the as-received material, is observed in the austenitic phase of the present aged DSS after fatigue [1]. On the other hand, the dislocation structure in the aged ferrite presents a band structure on $\{110\}$ and/or $\{112\}$ planes depending on the Schmid factor, **Fig. 3 a)**. The evolution of this band structure

near-surface of the notched area gives rise to the formation of microbands, which are oriented at 45° from the tensile direction and the interior of them are slightly disoriented with respect to the reference matrix, **Fig. 3 b)**. Moreover, EDX measurements have shown that inside these microbands a demodulation of the spinodal decomposition occurs [7].

SEM and AFM Observations. In the present aged DSS the electropolishing procedure to reveal phases, contrary to what was observed in the literature in as-received DSSs [8], showed higher



dissolution rate in the austenite than in the embrittled ferrite. Indeed, the austenite appears lower than the ferritic matrix **Fig. 4 a-b**). This fact may be attributed to the spinodal decomposed ferritic matrix. **Fig. 4 a)** gives an overview of the slip band distribution on both phases; in the austenite, the slip bands are fine and homogeneously distributed while in the ferrite are more dispersed and coarser. An interesting feature observed by AFM is that the extrusions in the aged ferrite do not appear as smooth as those in the austenite, **Fig. 4 c-e**). The analysis of the slip band profile shows that in the ferrite the average extrusion height is about 40 nm (with extreme values of 20 – 150 nm) while in the austenite the average is 90 nm (with extreme values of 30 – 150 nm). Moreover, in the ferrite phase the separation between extrusions are equivalent to the separation between microbands, about 5 μm . The aforementioned results suggest that microcrack nucleation is the result of the development of microbands in the near-surface region that have evolved from dislocation band observed in the bulk of the specimen. The misorientation between the microbands and the matrix could be explained by the formation of low-angle dislocation walls due to the reaction of two dislocation system gliding on a $\{110\}$ plane with two different Burgers vectors. From a such reaction a third dislocation would be formed with Burgers vector $[100]$ [9].

Summary

The study of surface damage and dislocation structure evolution in the S32750 duplex stainless steel in the aged conditions after fatigue has attained the following conclusions:

- a) Microcracks in the ferrite are the result of the developments of microbands in the near-surface region which lead to rough extrusions at the surface.
- b) Microbands are the result of the evolution dislocation bands observed in the specimen bulk.
- c) Roughness of extrusions in the ferrite is more pronounced than the observed in the austenite.

Acknowledgement

This work was supported by Agencia Nacional para la Promoción de la Ciencia y Técnica (ANPCyT) and Consejo Nacional de Investigaciones Científicas y Técnicas (CONICET) of Argentina.

References

- [1] I. Alvarez-Armas and S. Degallaix-Moreuil. *Duplex Stainless Steels*. ISTE Ltd, London, GB and J Wiley & Sons, Inc., Hoboken, USA; 2009.
- [2] H.D. Solomon, T.D. Devine Jr., in: R.A. Lula (Ed.), *Duplex Stainless Steels*, ASM, Cleveland (OH), 1983, p 693.
- [3] P.H. Pumphrey, K.N. Akhurst; *Mater. Sci. Tech.*, Vol. 6 (1990) p. 211.
- [4] A. F. Armas, S. Hereñú, I. Alvarez-Armas, S. Degallaix, A. Condó, F. Lovey; *Mater. Sci. Eng. A*, Vol. 491 (2008) p. 434.
- [5] A. Armas, S. Degallaix, G. Degallaix, S. Herenú , C. Marinelli, I. Alvarez-Armas; *Key Eng. Mater.*, Vol. 345/346 (2007) p. 339.
- [6] M. Balbi, M. Avalos, A. El Bartali, I. Alvarez-Armas; *Int. J. Fatigue*, Vol. 31 (2009) p. 2006.
- [7] S. Hereñú, M. Sennour, M. Balbi, I. Alvarez-Armas and A. F. Armas; *Duplex Stainless Steels Conference & Exhibition 13-15 of October 2010 Beaune, France*.
- [8] I. Serre, D. Salazar, JB Vogt; *Mater. Sci. Eng. A*, Vol. 492 (2008) p. 428.
- [9] J. P. Hirth and J. Lothe; *Theory of Dislocations*, J. Wiley –Sons, 1982, ISBN 0471-09125-1